Infrared adaptive optics system for the 6.5 m MMT: system status

M. Lloyd-Hart, G. Angeli, R. Angel, P. McGuire, T. Rhoadarmer, and S. Miller

Center for Astronomical Adaptive Optics, University of Arizona, Tucson, AZ 85721

http://athene.as.arizona.edu:8000/caao

Presented at the ESO topical meeting on
Astronomy with Adaptive Optics – Present Results and Future Programs
Garching bei München, September 7-11, 1998

Infrared adaptive optics system for the 6.5 m MMT: system status

M. Lloyd-Hart, G. Angeli, R. Angel, P. McGuire, T. Rhoadarmer, and S. Miller
Center for Astronomical Adaptive Optics, University of Arizona, Tucson, AZ 85721

Abstract

We report on the current state of the adaptive optics system being built for near infrared operation at the 6.5 m MMT. The system will use a single sodium laser beacon and a deformable secondary mirror to correct the telescope's imaging to the diffraction limit in the *H* band and beyond. The status of the telescope conversion project itself is also briefly covered. First light for the adaptive system is expected in mid 1999.

1. Conversion from MMT to 6.5 m

The old 6-mirror MMT was removed from its building over the summer of this year, and work has begun to construct the new telescope.[1] The optical support structure for the 6.5 m has very recently been installed (Figure 1). The primary mirror has been shipped from the Steward Observatory Mirror Lab where it was fabricated, to the MMT base camp at the foot of Mt. Hopkins. After polishing,[2] the rms surface error was 26 nm (Figure 2), corresponding to a Strehl ratio in the K band of 98%. A dummy concrete mirror has been placed in the telescope's primary mirror cell for a series of tests of the mirror support system and the telescope's elevation drive. The real glass mirror is expected to be put in place later in the year.

Figure 1. First view of the 6.5 m telescope installed in the old MMT building.

2. System Overview

Three key features of the system will maximize its scientific productivity. The laser guide star coupled to a large aperture telescope will allow the use of very faint guide stars for sensing of global image motion. The motion sensor will be an infrared detector in the main science dewar, to take advantage of the diffraction-limited image width, thus maximizing the sensor's sensitivity over the largest isoplanatic angle. Together, these features open up almost the entire sky to diffraction-limited imaging in the near infrared. Finally, throughput and emissivity at these wavelengths will be optimized through the use of an adaptive secondary mirror.

Figure 2. Interferogram of the 6.5 m primary mirror at 531 nm. The surface error after removal of 5 low-order Zernike modes is 26 nm rms.

A block diagram of the system is shown in Figure 3. After reflection from the primary mirror, aberrations in the wavefront are corrected at the deformable secondary, and the compensated beam is reflected to the Cassegrain focus. Here, a dichroic beamsplitter allows infrared light > 1 μm to pass into the ARIES high resolution infrared imager and echelle spectrograph. Visible light is reflected upward into the so-called "top box". This contains all the optics and detectors for measuring the instantaneous wavefront distortion. Readout from the wavefront sensor is used by a fast matrix multiplier hosted in a VME rack to compute corrections to the secondary mirror actuators.

The laser, attached to the telescope yoke, transmits a beam up the side of the telescope. The beam is folded along the telescope axis, and reflected via a fast steering mirror to a refracting launch telescope hidden behind the secondary mirror. A wedged window before the FSM reflects a small fraction of the laser light back to a diagnostic box which images both the laser pupil and far field onto an RS170 video camera.

Additional computers are coordinated over ethernet by the Adaptive Optics Data Server machine. The AODS is responsible for communication with the telescope control system, the real-time adaptive optics computer, the laser control machine, the user interface, and the science instrument ARIES.

3. Adaptive Secondary

The design of the adaptive secondary is illustrated in Figures 4 and 5. The control system is currently under construction by Media Lario in Lecco, Italy, using a glass shell and reference plate now being polished by the Steward Observatory Mirror Lab.

Voice coils in a hexapolar pattern comprising 336 actuators will be used to drive a 2 mm thick glass shell, 64 cm in diameter. Each actuator has an associated capacitive sensor which is used to measure the local displacement explicitly. A 50 mm thick plate of ULE glass, polished to a spherical surface with the same radius of curvature as the secondary itself, is used as the reference surface against which the shape of the thin mirror is measured. The back surface of the thin shell is aluminized, as well as the reflective front surface, to provide a common ground plane for all 336 capacitors.

Magnets glued to the back of the shell provide the field against which the current in the voice coil works. By using radially polarized annular magnets, we have been able to maximize the coupling between coil and magnet, which has reduced the mean power requirement by a factor of two compared to our original design, employing conventional axially polarized magnets. Heat generated by the coils' resistance is transferred up a cold finger to an aluminum heat exchanger where it is dumped into recirculating fluid piped in across the secondary spider vanes.

By using voice coils with local capacitive feedback, we avoid the problems associated with direct contact between the actuators and the deformable surface. For instance, thermal mismatches and delamination are not of concern. New problems present themselves however, and foremost amongst these is the need to convert the force actuators with zero stiffness into position actuators with essentially infinite stiffness. This is done through the capacitive sensors.[3,4]

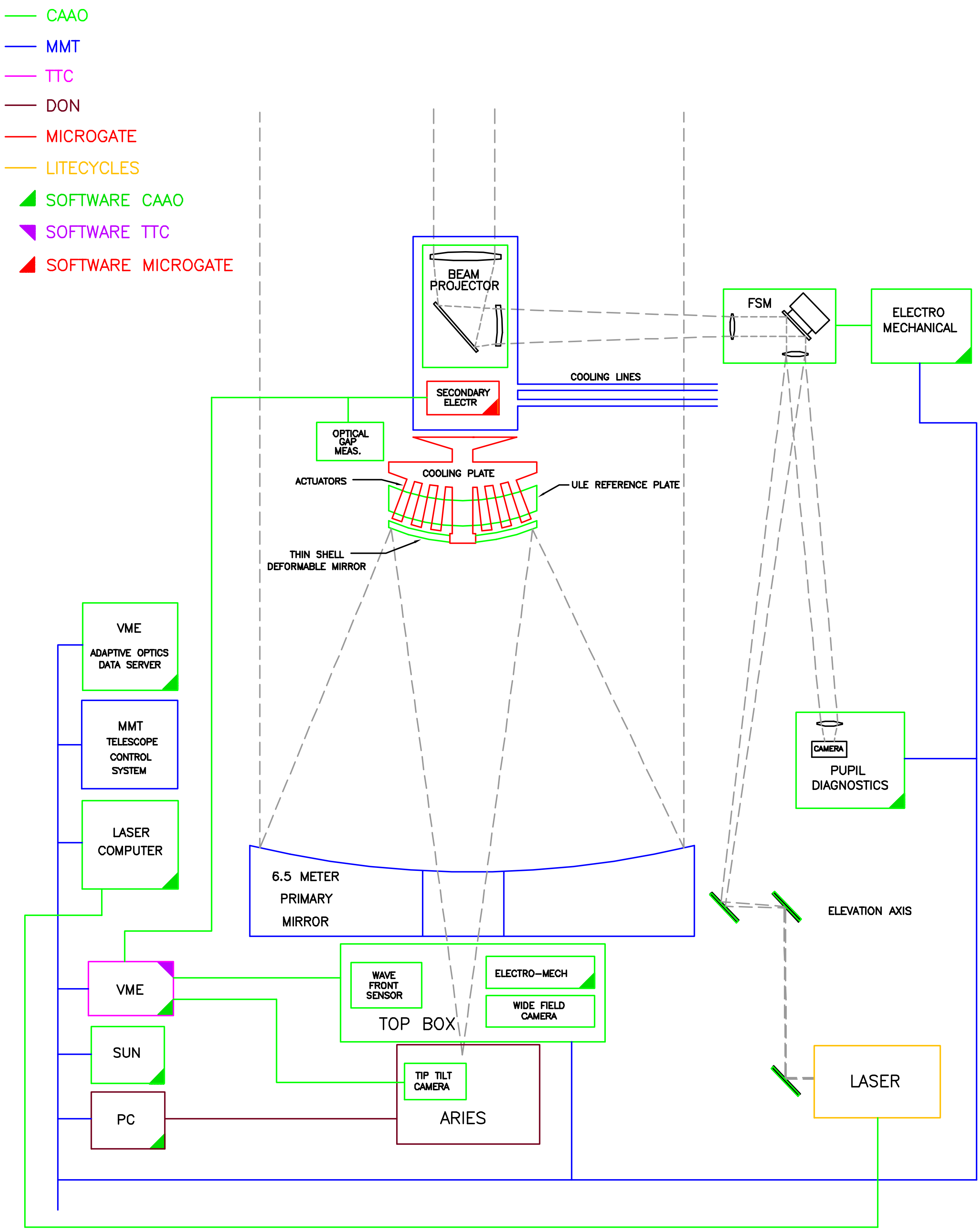

Figure 3. Block diagram of the 6.5 m AO system as it will be when fully-implemented.

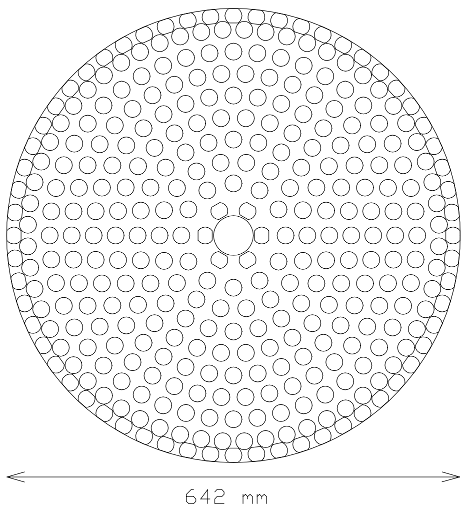

Figure 4. Hole pattern for the 336 actuators of the adaptive secondary. The circles represent the capacitive sensor pads that will be deposited on the ULE reference plate.

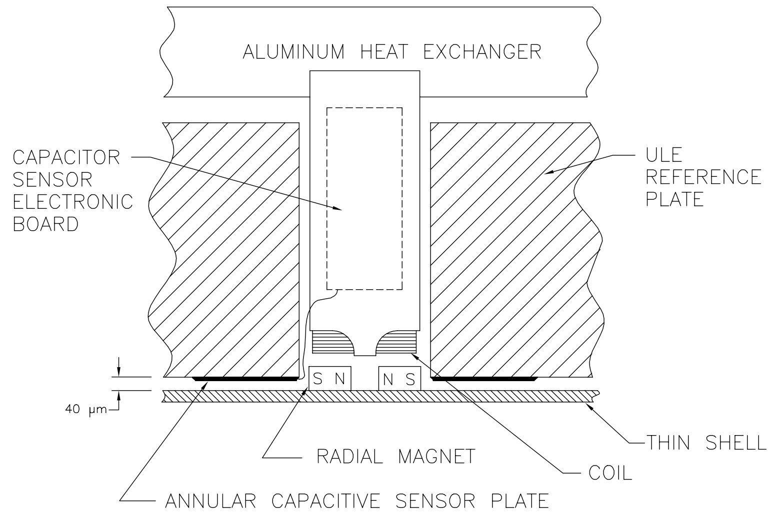

Figure 5. Schematic design of the voice-coil actuator assembly for the adaptive secondary.

The striking difference between operation with and without the local feedback is illustrated in Figure 6. A prototype adaptive secondary, almost full size at 55 cm diameter, has been constructed with 60 voice coil actuators.[5] When a single actuator is pushed without feedback (Figure 6*a*), by far the dominant effect is an overall tilt with some astigmatic bending. The tilt component of Figure 6*a* has been removed, but it is apparent in that in places, the local tilt was high enough to be immeasurable. There is no hint of a local bump. By contrast, in Figure 6*b*, capacitive feedback was applied so that actuators surrounding the one that was commanded to move work hard to stay in place. The expected local bump is now seen, with hints of dimples between the first and second rings of actuators.

a *b*

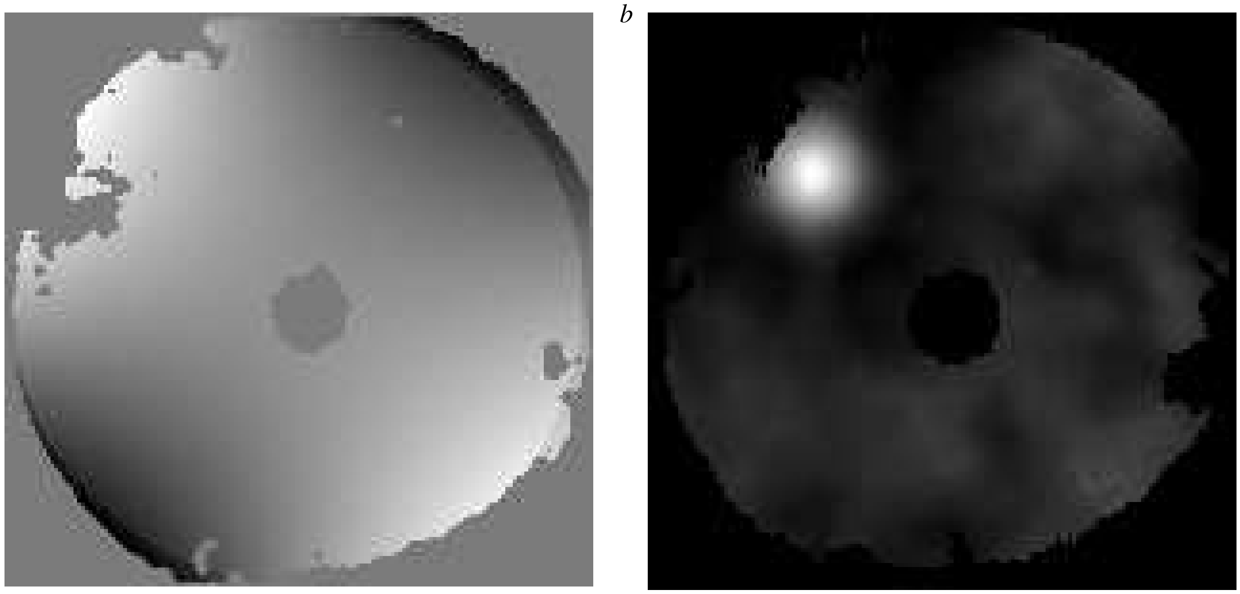

Figure 6. Phase maps of a 55-cm adaptive secondary prototype with 60 voice-coil actuators, showing the influence of a single actuator without (*a*) and with (*b*) feedback from the capacitive sensors.

4. Top Box

The wavefront sensing portion of the system is shown in the rendering of Figure 7. It is contained in a tub, referred to as the top box, 1.8 m in diameter that bolts directly to the instrument rotator at the telescope's Cassegrain focus. Visible light is fed into the top box by reflection off the dichroic entrance window to the infrared science dewar. Just before the *f*/15 focus, light can be diverted into a side-looking dewar containing a 2k $\times$ 4k CCD with a field of view of 66 $\times$ 132″. So that both the imager and the WFS can operate simultaneously, the camera can be fed by a choice of a pierced mirror or a selection of dichroics.

After the focus, light is folded onto a horizontal plane. An off-axis parabola collimates the beam, which passes through an atmospheric dispersion corrector and forms an image of the pupil on a steerable mirror. This mirror is used either to select a guide star in natural star operation, or to place the sodium beacon on the field stop of the WFS in laser mode. A second OAP refocuses the light onto the WFS, with the exit pupil at infinity. This allows the WFS to be translated between the focal positions for natural and laser guide star modes without affecting the mapping of the pupil onto the lenslet array.

The WFS itself is Shack-Hartmann sensor using a CCD39a 80 $\times$ 80 device from EEV with 24 µm pixels. The lenslet array, provided by AOA, is bonded directly to the CCD package. The lenslets are on a 144 µm pitch, commensurate with a 6 $\times$ 6 subraster of pixels. In normal use, the chip is binned by a factor of 3 to provide quad cell operation. Figure 8 shows the

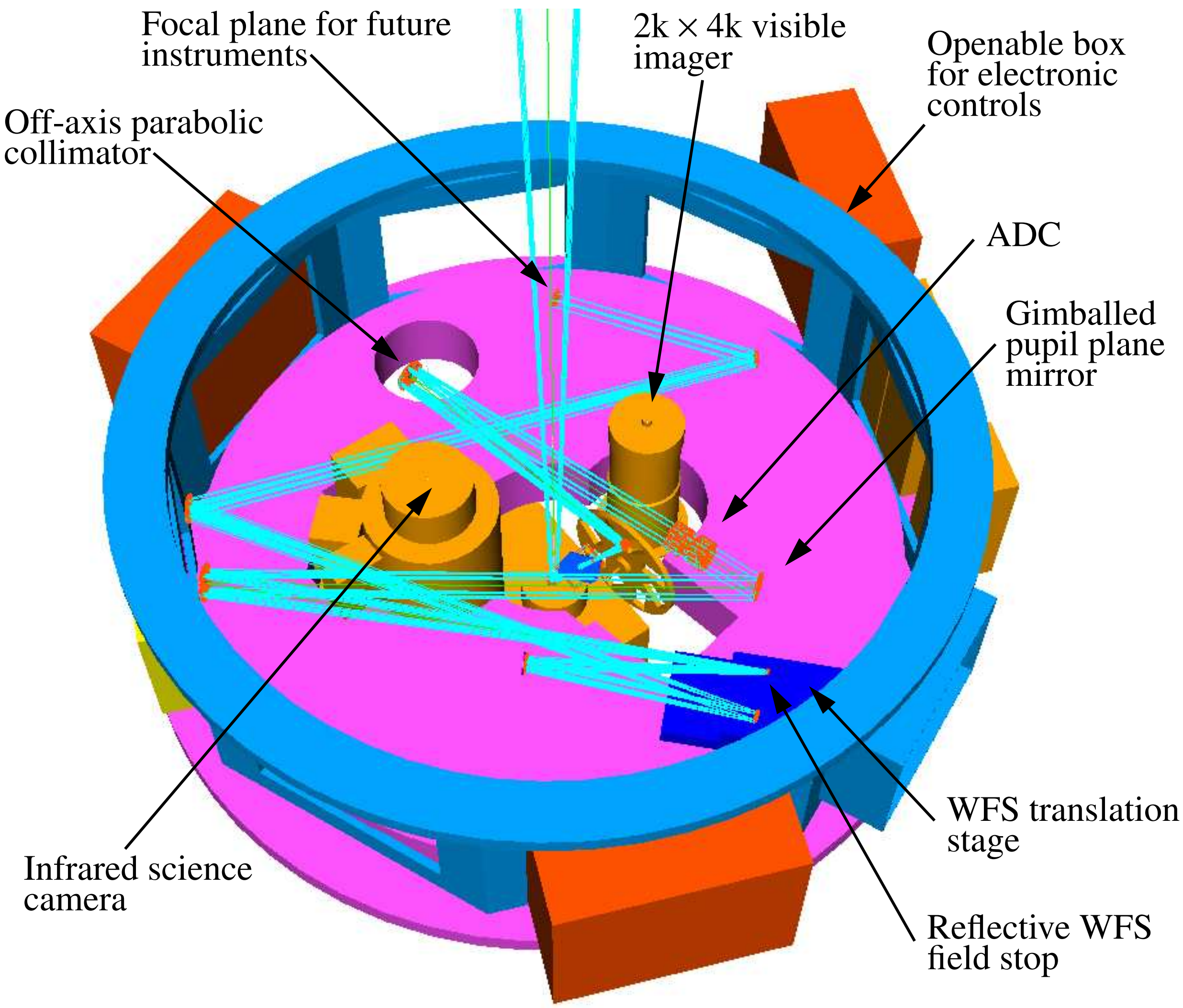

Figure 7. The view into the 6.5 m "top box", containing the wavefront sensor. Provision is also made for a number of visible light instruments including a wide-field camera, a separate narrow-field camera with very high resolution, and a spectrograph.

spots produced by the lenslet array on the CCD from a plane wavefront, immediately prior to gluing the two together. The excellent registration is shown in Figure 9, which shows the residual tilts registered by each quad cell. The worst mismatch between lenslet and CCD pixels produces a centroid vector 1.8 μm long, corresponding to 0″.037 on the sky. The rms is three times better – 0.7 μm, or 0″.013. These errors will contribute to the overall error budget by increasing the width of the final diffraction-limited image. In the *H* band, the diffraction limit of the 6.5 m is already 0″.05. Adding the registration error in quadrature will degrade this resolution by only 3%.

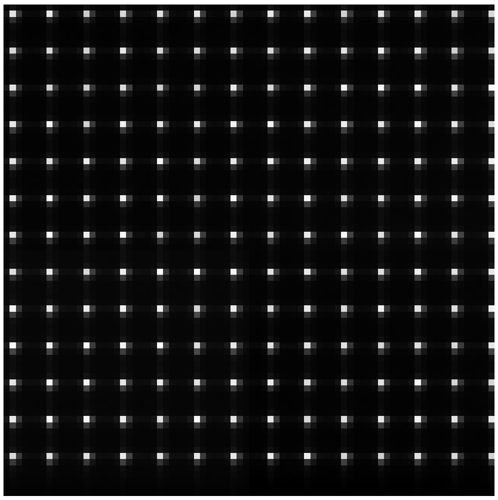

Figure 8. The WFS CCD illuminated with collimated laser light through a lenslet array tailored to match the pixel pitch.

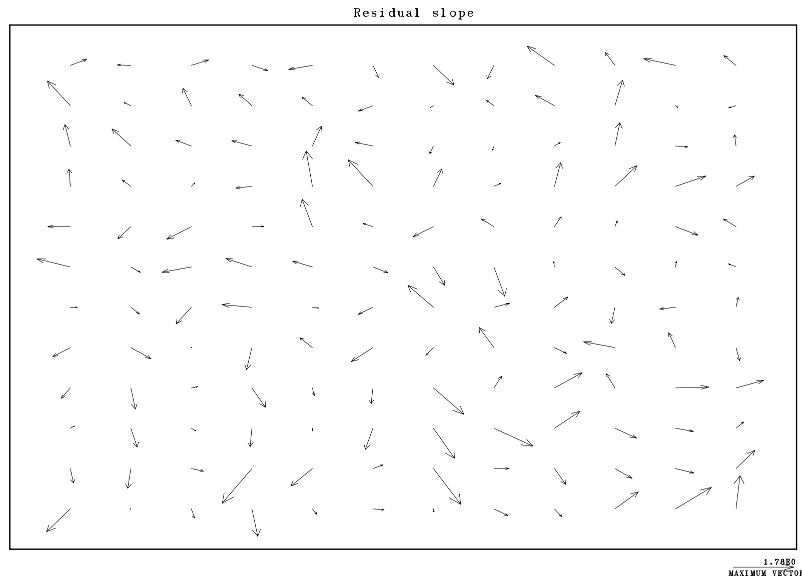

Figure 9. The slope errors measured by the WFS from the image in Figure 8. The longest vector is only 1.8 μm or 0″.037 long.

5. Sodium Laser

The laser, a solid state design being built by Lite Cycles of Tucson,[6] is expected to deliver 10 W at 589 nm with a wall-plug efficiency of about 5%. It uses Nd:YAG pumped by 120 W from continuous-wave laser diodes. The laser bandwidth is maintained at 700 MHz, well matched to the width of the peak in the doppler-broadened sodium absorption spectrum, by using a mode-locked design in the YAG cavity.

Light from the YAG at 1.064 μm is frequency doubled to 532 nm, then Raman shifted twice in a pair of $CaWO_4$ crystals, first to 560 nm, and then to 589 nm. In order to match exactly the absorption peak, the output of the YAG laser is tuned by cooling the crystal to 195 K. Frequency stability is maintained by servoing the temperature to the signal from a diode monitoring the output of a Fabry-Perot etalon which sees a small fraction of the outgoing laser light.

6. Test Facility

A facility is being constructed to allow complete closed-loop testing of the system outside the telescope environment. Figure 10 shows the arrangement which will initially be set up at the Steward Observatory Mirror Lab. A handling cart supports the top box and ARIES instrument in the same configuration as in the telescope. Two lasers within the top box generate light at 594 nm and 1.50 μm. After passing through a turbulence generator consisting of two rotating phase plates, both wavelengths are sent through beam expanding optics to the secondary, via two fold flats. There, a large doublet bends the light so that it appears to the secondary mirror to have come from the primary. After reflection off the secondary, the light is passed back down the beam train to the WFS and science camera. A criterion for optical design which has been met is that in the test facility, the image of the secondary on the lenslet array should have no more than 2 mm distortion at any point, compared to the image seen in the telescope.

The two separate wavelengths are used to simulate as closely as possible the situation in the telescope. A yellow HeNe laser with a wavelength only 5 nm different from the sodium D_2 line is used to simulate the return from the sodium beacon. The infrared light then models light from the tilt star. Since the two beams follow essentially the same path through the turbulence cell, focus anisoplanatism is the only significant source of error not included in the test.

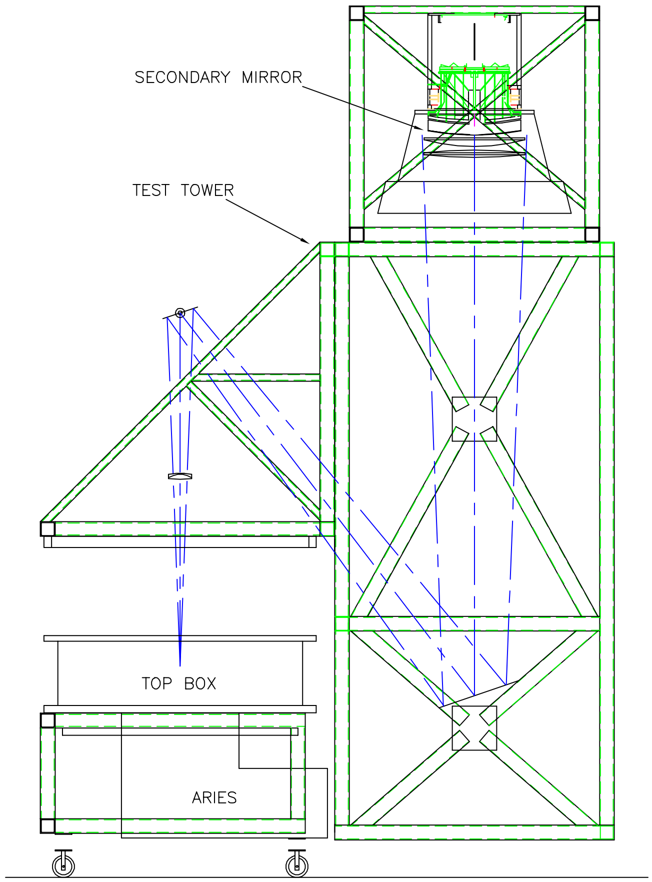

The infrared light source may also be used to measure the improvement in the point-spread function with the system running, by forming its image on the ARIES main camera.[7] In addition, a phase-shifting interferometer is included in the top box to allow explicit measurements of the shape of the secondary mirror in response to static or dynamic commands from the user.

After extensive system tests in the lab, the entire test facility will be transported permanently to the telescope, where it will continue to provide support for system tests that need not impact the telescope's schedule. The facility will also double as storage for the secondary and Cassegrain instrument when they are not in use.

The large doublet directly beneath the secondary mirror has been designed so that it may also be installed in the telescope with the rest of the AO system. This will allow complete system tests *in situ* during the day, or during periods of inclement weather.

Figure 10. Elevation of the test facility as it will be installed at the MMT.

7. Phased Implementation

This is a very ambitious project, which clearly cannot be brought to completion in one single step. The system's full functionality will be implemented in four phases:

1. Set up a simplified system in the Mirror Lab which allows us to close the loop on artificial turbulence using the test facility. (June 1999)
2. Transfer the system to the mountain. Verify system performance on natural guide stars. (November 1999)
3. Add the laser, the global tilt sensors, and associated additional electro-mechanical controls. Verify performance in sky tests. (March 2000)
4. Begin to add further infrared science instruments, such as the 10 – 20 µm MIRAC array camera and the near infrared FSPEC spectrograph.

8. Summary

The AO system described here has been designed to be an integral part of the telescope it serves, rather than an add-on. This approach, which has great benefit to the throughput, emissivity, and observing efficiency has been greatly facilitated by the concurrent construction of the adaptive optics and the telescope itself. The realization of the adaptive secondary, the 10 W sodium laser beacon, and the infrared tilt sensor will make the 6.5 m a superb instrument for observing faint objects essentially anywhere in the sky.

9. Acknowledgements

Work described here has been supported by the Air Force Office of Scientific Research under grant #F49620-94-1-0437 and grant #F49620-96-1-0366, and by the NSF under grant #92-03336. We thank R. Sarlot, B. Fitz-Patrick, M. Rademacher, B. Jacobsen, T. Roberts, and J. Burge for their help with some of the work presented here. Thanks to Bill Kindred of the MMTO for figure 1.

10. References

1. S. West et al. “Toward first light for the 6.5-m telescope,” *Proc. SPIE conf. on Optical Telescopes of Today and Tomorrow,* ed. A. Ardeberg, **2871**, 1996

2. H. M. Martin et al., “Fabrication and measured quality of the MMT primary mirror,” *Proc. SPIE conf. on Advanced Technology Optical/IR Telescopes VI*, ed. L. M. Stepp, **3352**, 1998

3. T. K. Barrett et al., “Adaptive secondary mirror for the 6.5-m MMT,” *Proc. SPIE conf. on Adaptive Optical System Technologies*, ed. D. Bonaccini & R. K. Tyson, **3353**, 1998

4. G. Brusa et al., “Optical testing results of a reduced-size adaptive secondary prototype,” *Proc. SPIE conf. on Adaptive Optical System Technologies*, ed. D. Bonaccini & R. K. Tyson, **3353**, 1998

5. D. G. Bruns et al., “Final prototype design for the adaptive secondary mirror of the 6.5-m MMT,” *Proc. SPIE conf. on Adaptive Optics and Applications,* ed. R. K. Tyson & R. Q. Fugate, **3126**, 164-172, 1997

6. J. T. Murray, “Sodium guide star laser for the 6.5 m MMT telescope,” in *ESO Workshop on Laser Technology for Laser Guidestar Adaptive Optics Astronomy*, Garching, 1997

7. D. W. McCarthy, J. H. Burge, J. R. P. Angel, J. Ge, and B. C. Fitz-Patrick, “ARIES: Arizona infrared imager and echelle spectrograph,” *Proc. SPIE conf. on Infrared Astronomical Instrumentation*, ed. A. M. Fowler, **3354**, 1998